Grand Libreville (Gabon) coastline machine learning and convolutional neural network detection and automatic extraction of the methods

Nina Manomba-Mbadinga, Simona Niculescu, Narimane Zaabar, Jean-Bernard Mombo, Guanyao Xie

Grand Libreville (Gabon) coastline using machine learning and convolutional neural network detection and automatic extraction of the methods

Nina Manomba-Mbadinga [a,*], Simona Niculescu [a-b], Narimane Zaabar [a], Jean-Bernard Mombo [c], Guanyao Xie [a]

[a] University of Western Brittany, CNRS, LETG Brest UMR 6554 CNRS, Technopôle Brest-Iroise, Av. Dumont d'Urville, Plouzané-Brest, Institut Universitaire de France (IUF) [b], Omar Bongo University, LAGRAC, Dept of Geography, Environmental and Marine Sciences,680 avenue President Léon Mba, BP 13131 Libreville [c]

ABSTRACT

Coastal erosion is a major problem that has been worsened by climate change, along with other natural occurrences like droughts and marine flooding. Countries situated along coastlines are facing significant challenges when it comes to preserving their land and protecting their people and assets. To mitigate the damage caused by the encroachment of the sea on land, effective monitoring tools and methods are required. Several remote sensing techniques and methods have been developed to address these issues, including machine learning and deep learning methods. In this study, object-oriented analysis (OBIA), pixel-oriented analysis (PBIA), and convolutional neural network (CNN) methods are used to automatically detect and extract the Greater Libreville coastline, based on Pléiades very high-resolution satellite image dating from 2022. Three test areas were chosen there and then extracted. The first zone is located in the north of the municipality of Akanda (marked by the presence of small coastal cliffs). The second zone is located in the commune of Libreville (sandy beach). The third zone is located in the municipality of Owendo (artificialized beach, mostly muddy). The images of the three zones were the subject of a classification based on the methods mentioned above. Results of proposed methodologies showed competitive Overall accuracy (OA) values obtained with OBIA method and the CNN model. However, the OBIA method using Random Forest algorithm (RF) achieved the highest accuracy rates, which reached 95%, 90%, and 80% for the 3 test areas respectively.

Keywords: Remote sensing, machine learning, deep learning, Grand Libreville, coastal erosion, OBIA_PBIA, RF, SVM, CNN

1. INTRODUCTION

Artificial intelligence (AI) is an essential tool of the current era. It is present everywhere, both in our homes and outside. Although AI is somewhat controversial because it is seen as an adversary to humans, it is proving to be a revolution for humanity in several areas. Machine learning (ML) and deep learning (DL) are subfields of AI that offer many algorithms that are widely used in various professional fields on different topics. Geomatics deals with various related subjects, such as human activities, agricultural plots, drought and coastal erosion monitoring, and various other human pursuits. It has been able to integrate ML and DL using robust and reliable algorithms. The ML algorithms include decision trees (DT), the k-nearest neighbors (K-NN) algorithm, linear regression, the Naïve Bayes algorithm,

logistic regression, gradient boosting, forests (RF), and the support vector machine (SVM). On the other hand, DL integrates several algorithms such as, convolutional neural networks (CNN), recurrent neural networks (RNN), radial basis function networks (RBFN), long-term and short-term memory networks (LSTM), iterative adversarial networks (GANs) and restrictive Boltzmann machines (RBM).

Coastal erosion is a topical issue that has been the focus of renewed attention for several decades. “Coastal areas will see continued sea level rise throughout the 21st century, contributing to more frequent and severe coastal flooding in low-lying areas and coastal erosion. Extreme sea level events that previously occurred once in 100 years could happen every year by the end of this century”. Given this reality, several developed countries have conducted decades of research to find solutions to this problem. While several developing coastal countries are struggling to assess the evolution of their coast. In this study, which deals with the detection and extraction of the Greater Libreville coastline, machine, and deep learning methods were used, including random forest (RF) and support vector machine (SVM) for machine learning and CNN for deep learning. These are considered to be among the most effective classification methods. Nevertheless, opinions differ on their accuracy, even though their reliability is undisputed. Some studies confirm the similarity of classification accuracy between random forest and support vector machine ([1], [2]). However, studies ([3], [4], [5]) believe that SVM outperforms RF. Conversely, other studies ([6], [7], [8]) tend to believe that RF performs better than SVM. As for CNN, according some studies [9], [10] give more satisfactory results than RF and SVM. In this paper, we evaluated the performance of these different approaches for the detection and extraction of the Greater Libreville coastline using Pléiades very high-resolution image from 2022. For this comparison, we selected the models whose relevance was based on the parameterization of the number of trees (Ntree) and the number of variables (Mtry) for the RF, the cost value (C), and the gamma (γ) penalty function for the SVM, the scale and homogeneity for the CNN.

2. Study area

The Grand Libreville town is composed of four municipalities (Figure 1), namely Libreville, Ntoum, Owendo, and Akanda. The area is situated within the coastal sedimentary basin of Gabon, which is characterized by low altitudes. Three study areas were selected in the coastal municipalities of Greater Libreville to apply the proposed methodology. The first area is located in the municipality of Akanda and covers an area of about 5 km. It is covered with shrubby vegetation and characterized by small discontinuous coastal cliffs. In addition, the beach is essentially characterized by an extension of the reef flat towards the sea and covered with a thin layer of sand. The second one, located in Libreville, is more urbanized and extends over approximately 4 km. Its projecting sandy beaches leave rocky outcrops in some places. This sector is part of the heart of the capital and boasts many infrastructures, including roads, schools, hotels, restaurants, and residences located along its sandy beaches. The third area, located in Owendo, is an urbanized area that stretches for about 13 km.

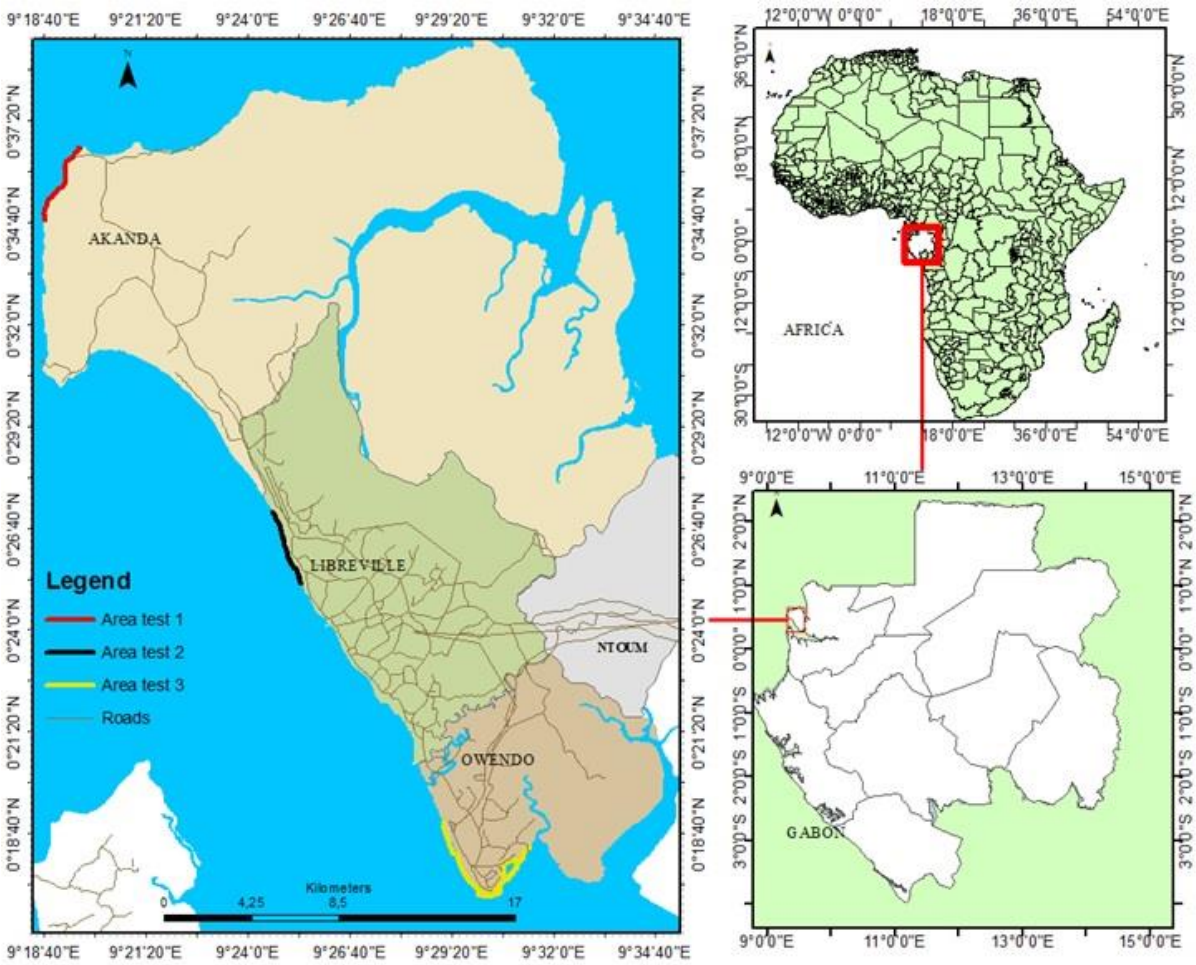

Figure 1: Geographic situation of the study area

3. Methodology

To address the assigned purpose of this study, the proposed methodology includes the following steps: the choice of the baseline of the coastline, the choice of data, the processing tools, and the processing methods.

There are about 45 coastline indicators [11] depending on the type of coast around the world. The vegetation limit, the outer limit of coastal construction, the run-up limit, and the limit between the dry sand and the wet sand are the references used for the characterization of the coastline of our three test zones.

3.1 Materials

Both open-source and paid software were used, these are QGIS, Orfeo tool box (OTB), ArcGis, and eCognition. QGis (version 3.28.4) was used for image preprocessing, image segmentation, and cartographic presentation of our input data (images and samples). OTB (version 8.1.1) was useful for the generation and prediction of RF and SVM

classification models for both PBIA and OBIA approaches. ArcGis (version 10.8.1) on the other hand was used to generate the training and verification points selected according to the characteristics of the images randomly. These data are very important for the application of the different methods. Also, ArcGis was used for the extraction of the coastlines of our different areas of interest as well as the layout of the final cartographic results. To carry out the image classification through CNN, we used eCognition software version 10.0.

3.2 Machine learning approaches

Two machine-learning algorithms were established and compared: RF and SVM. The objective was to define the most efficient one for the accurate detection and extraction of the coastline. These algorithms were applied in two image levels according to PBIA approach based on pixels and the OBIA approach based on image segmentation.

The pixel-based image analysis approach is a process that consists of classifying each pixel of an image directly according to its spectral similarity. It was tested using OTB software for shoreline detection. Five steps were followed: identification of thematic classes, model training, classification, accuracy assessment, and shoreline extraction (Figure 2). In this context, we decided to classify our image into five classes as previously defined. For each class, at least, 200 samples were created using ArcGIS software. Of the samples, 80% were used in the training phase, and the remaining 20% were used for the crucial validation phase. It was imperative to use the input data, which is the very high-resolution Pléiades image and the training and validation samples, to test the robustness of the random forest (RF) and the support vector machine (SVM) for the classification pixel by pixel (figure 2).

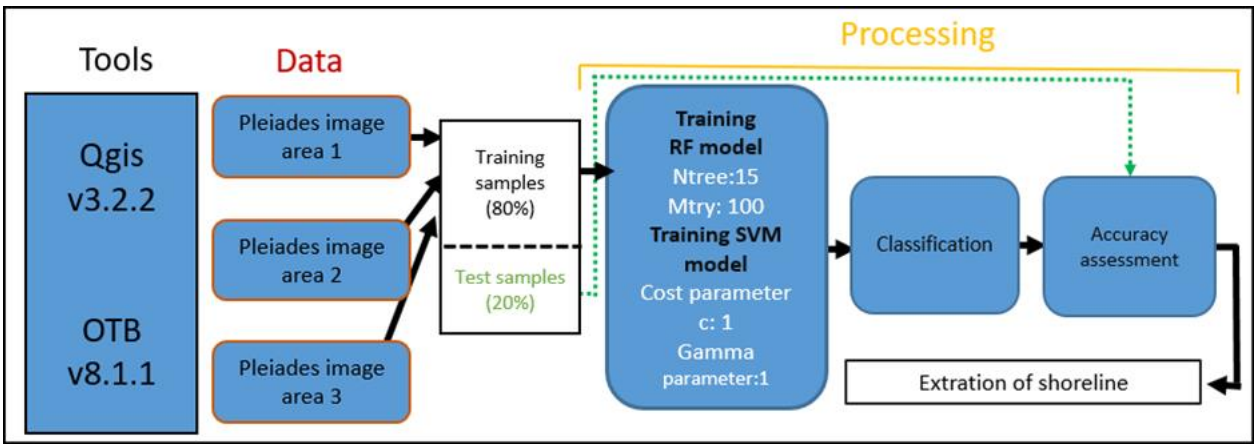

Figure 2: Shoreline extraction by PBIA approach

Object-based image analysis (OBIA), on the other hand, is based on the fundamental principle that an image is not made up of pixels but of several objects. Objects are created based on similarity criteria built on the spectral response, texture, and neighbourhood. The eCognition software was the main tool used to perform this analysis. This approach is almost identical to the previous one, with one difference: the segmentation phase. Segmentation is a crucial step that strongly influences the classification quality. The scale parameter in multiresolution segmentation is key to controlling

the size of the segmented objects, and should be optimized for improving OBIA classification [12]. There are a variety of segmentation algorithms. For this study, multi-resolution [13] segmentation algorithm was selected, making it possible to extract some relevant information (figure 3).

Random Forest is an algorithm built into the OTB software. Build multiple decision trees using a randomly selected subset of samples and learning variables. It is one of the most successful classifiers in machine learning. It has many advantages, such as high-precision output [14]. Despite the robustness of radio frequency, it also has some obvious disadvantages, such as tree visualization, due to the use of multiple trees for prediction [15]. Its classification division rules are ambiguous, so it is considered a black-box classifier [14]. The Ntree and Mtry are the two parameters that strongly influence the RF. They are user defined. The influence of these parameters on the different precision and the Mtry parameter is more significant than the Ntree parameter [16]. Nevertheless, the use of the optimal values for the two parameters is essential to obtain a better precision. Belgiu and Drăguţ [17], proposed 500 as the default number for Ntree. Along the same lines**,** Guan and al [18] advise as many Ntree values as possible, indicating that the RF classifier is efficient/robust and resistant to overfitting. Regarding the Mtry parameter, it is usually defined as the square root (sqrt) of the number of input variables unlike other researchers who intend it to be equal to the total number of available variables [16]. The opinion of Belgiu and Drăguţ [17] is completely opposite and asserted that setting such a value can however affect the speed of the algorithm because the method has to calculate the information obtained from all the parameters expressed to split the nodes.

In this work, we assigned the values of 15 and 100 respectively to Ntree and Mtry after several tests. This setting was maintained for each of the study areas. After training the model and passing it through the classification phase, we tested its reliability, and for this, 20% of the samples were used to produce the matrix and calculate the Kappa coefficient and the overall accuracy (Overall Accuracy) on OTB (Figure 3). Then the image, which was in the raster file, was converted to a vector file. The last step was the extraction of the coastline.

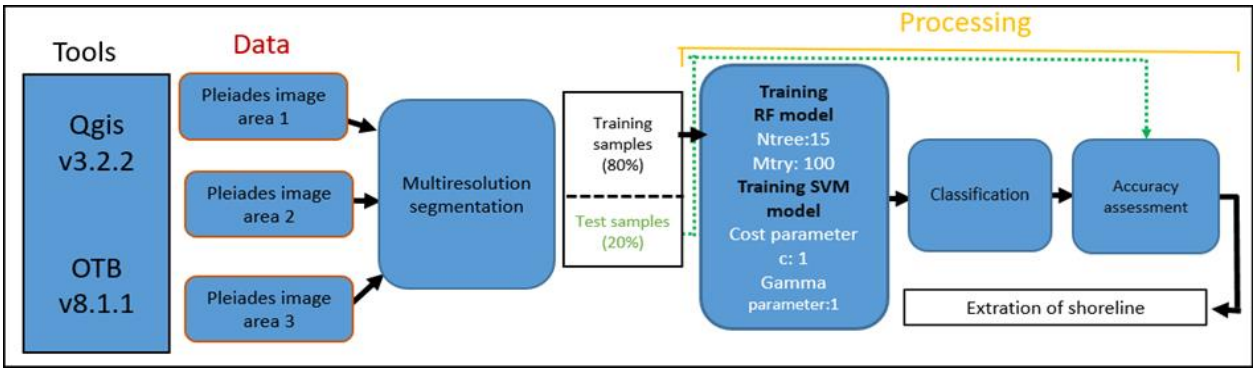

Figure 3: Shoreline extraction by OBIA approach

Another algorithm was tested, it's the support vector machine (SVM). It is a supervised machine learning classification algorithm [19]. It is a linear classifier. It is part of the most powerful machine learning (ML) algorithms. The basic principle of SVM is to reduce a classification or discrimination problem to a hyperplane (feature space) in

which the samples are separated into several classes whose boundary is as far as possible from the data points (maximum margin) [20].

Several kernels, such as linear, polynomial, Gaussian radial basis function, and sigmoid kernels can be used in SVM models.. The cost parameter C and the gamma parameter are the two main parameters that can significantly affect the performance of the SVM. RBF is the most popular used in support vector machines. In this work, the linear kernel was applied and the default values of two parameters were maintained, namely 1 for each of the parameters.

3.3 Convolutional neural network (CNN)

The CNN architecture was created in Trimble eCognition Developer (v.10). The CNN Training process consists of three main steps: 1) creating patch samples, 2) generating and training the model, and 3) applying the model. To this process is added that of classification based on the Object-Based Image Analysis (OBIA) (Figure 4). First, it would like to point out that the convolutional neural network is a deep learning (DL) model inspired by the architectures of biological neural networks. This model is inspired by the ability of the human brain to detect and process text, images, and videos. CNN is composed of neurons with learnable weights and biases [21].

As input, convolutional layers use patches of image samples containing all the features by scanning the entire image. The first convolution layer detects image features such as edges, shapes, and textures. Subsequent layers then detect more complex features based on the features detected by the previous layer. A fully connected layer that combines the features detected by the convolution layers and uses them to classify the image usually follows the last convolution layer.

Several parameters are crucial for CNN optimization. Tuning the sample patch size, hidden layers and learning rate are essential steps to obtain a performing model. Thus, in order to choose a relevant sample patch size, we took into consideration the dimensions of our five target classes (Water, wet sand, dry sand, vegetation, and urban). Since the patch sample size is considered one of the most critical parameters in the optimal CNN architecture [22], several sample sizes were tested: 8×8, 10×10, 16×16, 20×20, and 32×32 pixels. After having followed a cross-validation process, the CNN models of our three test images (Akanda, Libreville, Owendo) were fed with the 20×20 sample patch size; 8×8 and 20×20 pixels respectively. In total, the global number of labeled sample patches for training the models of the images Akanda, Libreville, and Owendo are respectively: 5000, 10000, and 10000.

Once the sample patches have been created, the next step is to create the CNN model. In this process, all spectral bands of the input data have been solicited. Two hidden layers were constructed for each CNN model after running cross-validation and evaluating the CNN output accuracy results. The maximum pooling was applied. Then following a cross-validation method, a convolution was implemented. The models of the images of the Akanda and Owendo areas were parameterized so that the kernel size value of the first layer is 5 × 5 and 7 × 7 for that of the second layer. While the second model, the one generated from the Libreville area image has a kernel size of 3x3 for the first and second layer.

In training step of CNN model of Akanda area, the following parameters were retained: patch size of 50 and 5000 training steps. From a cross-validation process revealed that the optimal learning rate to be set at 0.0006. This made it possible to achieve a good performance. The same configuration was assigned in the case of CNN architecture of the two other areas. Moreover, after several cross-validation processes (with rates set at 0.0008, 0.0006, 0.0005, 0.0003 and 0.0001), their optimal learning rate retained was 0.0001 each. Note that if the learning rate is insufficient, it can either increase the time of the learning process (at low rate), this could block the network in the local minima, or reduce it (at a high rate), but it is could then, in this case, that the network does not reach the minima. In both cases, it would be impossible to obtain correct weights.

The application of the CNN generated from the three images allowed to obtain three thermal maps were generated based on fully connected layers. The layers correspond to the occupation of the ground according to the five predefined classes. These heatmaps have a unit for each class predicted by CNN where two possibilities were considered: a value close to 1 or a value close to 0. The first case would indicate a higher probability of the category, while the second case would indicate a probability weaker.

The results of the training of the built models of the three zones images served as input datasets for the OBIA classification. The latter is dedicated to the development of automated methods for the segmentation of geospatial imagery into image objects. Since the CNN is carried out at the pixel level, the OBIA approach will be applied to it so that the entirety of this image is transformed into a segmented object image from the multi-resolution algorithm [23].This last is a widely used segmentation algorithm for very high spatial resolution data applications. It is based on the evolution of the fractal network and aggregating individual pixels into objects of increasing size at several levels in an iterative process. Critical MRS issues are parameter optimization and segmentation quality assessment. This segmentation process is based on three parameters whose adjustment is submitted to the user. Mainly: 1) the scale, (defined as the maximum allowed heterogeneity within the objects); 2) the shape (weight between the spectral and a shape factor); and 3) compactness (regularization factor). After cross-validation, the scale, Shape and compactness parameters were set to: 20, 0.9 and 0.1 respectively for the images of our three areas of interest. The resulting objects were trained and classified based on a combination of neighborhood, spatial properties, and similarity in CNN probability. After final classification, the polygon vector images obtained were converted to polyline format in order to detect and extract the target shoreline on each of the images. The selected coastlines are the limit of the run-up, the limit between dry sand and wet sand, the limit of vegetation on the sea side as well as the limit on the land side of protection works. In fact, the extraction is done by selecting the class identifier of interest in the attribute table and eliminating all other class polylines (figure 4).

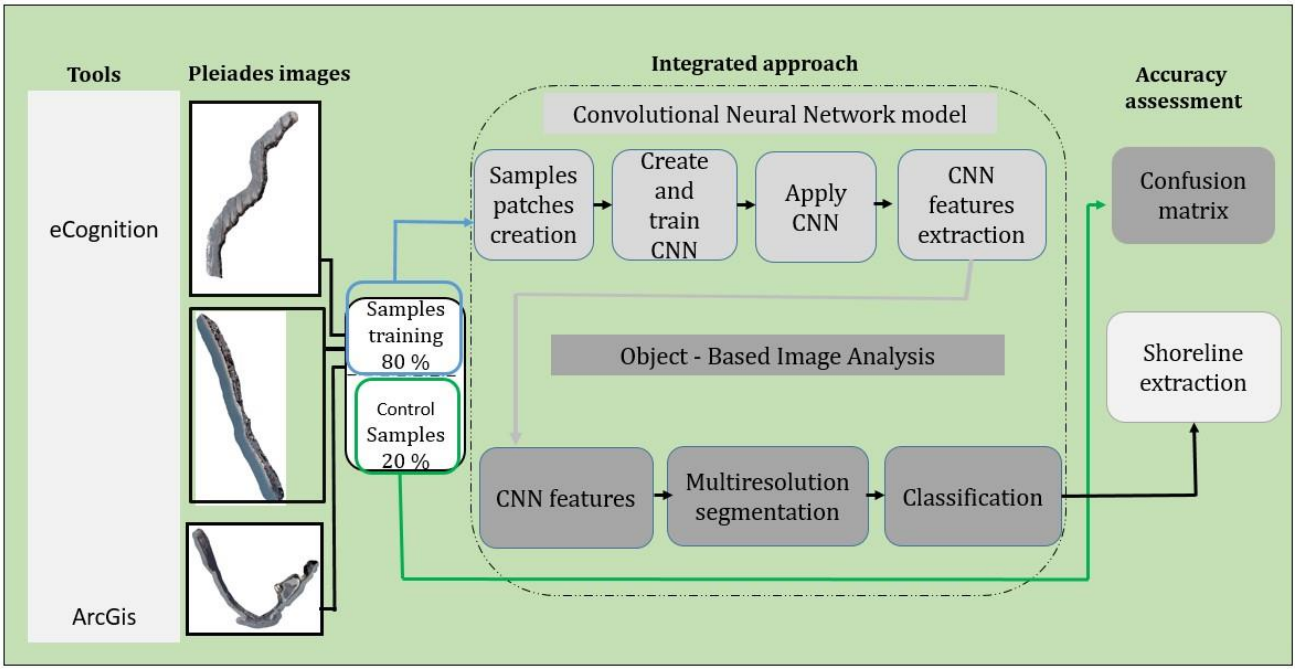

Figure 4: Shoreline extraction from CNN integrated with OBIA

3.4 Accuracy assessment

Through precise evaluation, the reliability and relevance of the comprehensive method for shoreline extraction in the three test areas developed in this study can be assessed. The accuracy assessment is based on precision indices generated by the confusion matrix, namely OA, Kappa index and all other precision indices by class (class precision, class recall and class F-score). A visual inspection was also performed. To form the confusion matrix for each image of the different test regions, the result of the classification was crossed with the 20% sample dataset manually created by "Edit function" (ArcGis). This approach is applied based on the "ComputeConfusionMatrix" process on OTBv8.1.0.

3.5. Data

3.5.1 Pleiades

The methodology followed in this study was applied to three Pléiades satellite images acquired on 21 and 27 August 2022, and provided by Airbus DS. The images available with high spatial, multispectral, and panchromatic resolution have four bands: red, green, blue, and near-infra-red. The precision of this image is 2 meters (Table 1). The projection system of the study areas is (WGS 84 32 N).

Images	Acquisition day	Precision (m)	Resolution (m)
Pléiades _PHR1A Akanda	2022-08-27	2	4 spectral bands: visible Red, Green, Blue and Near infrared (RGB and NIR)
Pléiades_PHR1A Libreville	2022-08-21	2	4 spectral bands: visible Red, Green, Blue and Near infrared (RGB and NIR)
Pléiades_PHR1A Owendo	2022-08-27	2	4 spectral bands: visible Red, Green, Blue and Near infrared (RGB and NIR)

Table 1: Pleiades characteristic

Previously, these images went through a pre-processing phase to improve their visual quality (figure5). First, the images collected were georeferenced using the "georeferencing" tool. Georeferencing allows the user to define the location of rasters to be georeferenced in their spatial location based on geographic coordinates. In our case, a satellite image of Greater Libreville dating from 2013 was used as a base. Then; the images were mosaicked using the “mosaic” algorithm. Tiling allows multiple rasters or images from the same sensor to be merged into a single overview image. At another time, this mosaic underwent an orthorectification. An ortho-rectification is a process allowing correct the geometry of the images in order to make them superimposable with other rasters. Finally, our three different areas of interest were extracted from this mosaic from the Polygon Shapefiles representing the companies in the areas. The "raster" tool was used for this purpose.

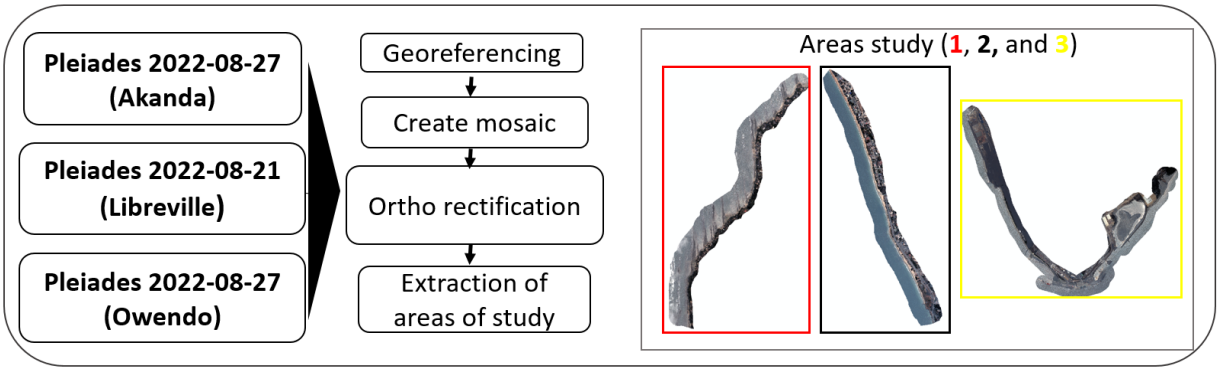

Figure 5: Pre-processing of images

3.5.2 Samples creation

Furthermore, other data just as necessary as the previous ones have been collected. These are the training and validation samples. These samples provide information about the surface characteristics of the area studied. They are labelled and organised into classes. In our case, five classes were retained, namely: water, wet sand, dry sand, vegetation, and urban (figure 6).

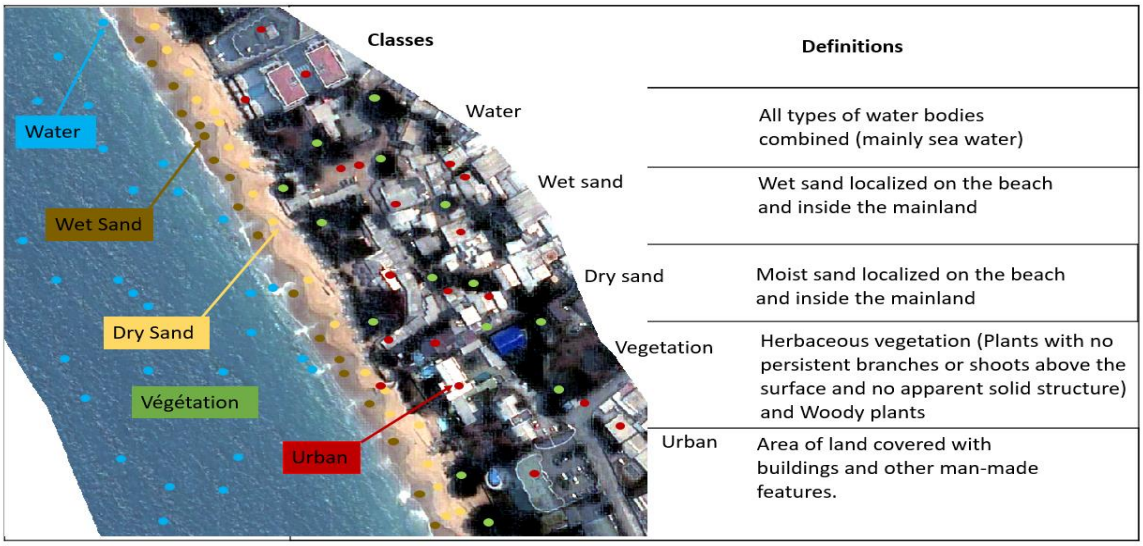

Classes	Definitions
Water	All types of water bodies combined (mainly sea water)
Wet sand	Wet sand localized on the beach and inside the mainland
Dry sand	Moist sand localized on the beach and inside the mainland
Vegetation	Herbaceous vegetation (Plants with no persistent branches or shoots above the surface and no apparent solid structure) and Woody plants
Urban	Area of land covered with buildings and other man-made features.

Figure 6: Creation of samples

As with the type of algorithm chosen, the quality and number of classified samples has a significant impact on the accuracy of the expected result (land cover map). The selection of samples is therefore a crucial step. Controversy over the size of these samples exists in the scientific community. For some, to obtain good classification accuracy, the training data must represent 0.25% of the total study area [24]. In contrast, others argue that training samples should not be less than 10 times the number of features in the classification model [25]. Never mind, you have to choose a large number of samples to improve the results.

Two hundred (200) train samples were created for each class in the three test zones. We took care to ensure that these points did not overlap. We then converted these points into polygons (squares) to form the various models. Each sample was labelled according to the class it belongs to.

4. Results and discussion

The results presented within the framework of this study come from the application of three approaches, which are the PBIA, the OBIA and the CNN. The first two approaches were designed from models based on two algorithms: RF and SVM. As for the CNN, it was combined with the OBIA approach. Given the diversity of the results obtained, the analysis will be based on the results of the approach that demonstrated the best performance rates for the classification of the three test areas located respectively in the municipalities of Akanda, Libreville and Owendo. 15 classified images from the three different approaches were obtained. Each algorithm was tested on the three test areas. As well as with the PBIA and OBIA approaches, the RF recorded the best classification performance rates but those obtained from the RF-OBIA are the most relevant (Table 2).

.

	PBIA		**OBIA**		
	RF	SVM	RF	SVM	CNN
Zone 1 (Pléiades_Akanda)	OA : 87 % Kappa : 83 %	OA : 86 % Kappa : 82 %	OA : **95** % Kappa : **94** %	OA : 92 % Kappa : 90 %	OA : 91 % Kappa : 88 %
Zone 2 Pléiades_Libreville)	OA : 89 % Kappa : 86 %	OA : 79 % Kappa : 74 %	OA : **90** % Kappa : **88** %	OA : 82 % Kappa : 77 %	OA : 68 % Kappa : 75 %
Zone 3 Pléiades_Owendo)	OA : 80 % Kappa : 75 %	OA : 79 % Kappa : 74 %	OA : **80** % Kappa : 75 %	OA : 67 % Kappa : 58 %	OA : 79 % Kappa : 74 %

Table 2: comparison of the performance of ML and DL algorithms

OA and kappa values of the image classifications of the three zones are respectively: 95% and 94% for the Akanda zone; 90% and 88% for the Libreville area and 80% and 75% for the Owendo area. Overall, SVM-OBIA was also achieved satisfactory results. It showed OA index and kappa index rates of 92% and 90 for the Akanda area; 82% and 77% for the Libreville area and 67% and 58% for the Owendo area. The approach having been the least efficient for the classification of the coastline of the three images of the test areas is the CNN. The OA and the recorded kappa indices are respectively: 91% and 90%, 68% and 75 and 79% and 74%.

Of the 15 images resulting from the tests of the different approaches, only three images will be presented zone (1, 2 and 3). These are the resulting classification images from the RF-OBIA. The figures below (figures 7, 11 and 13) present in each case the image of the study area and then the result of its classification

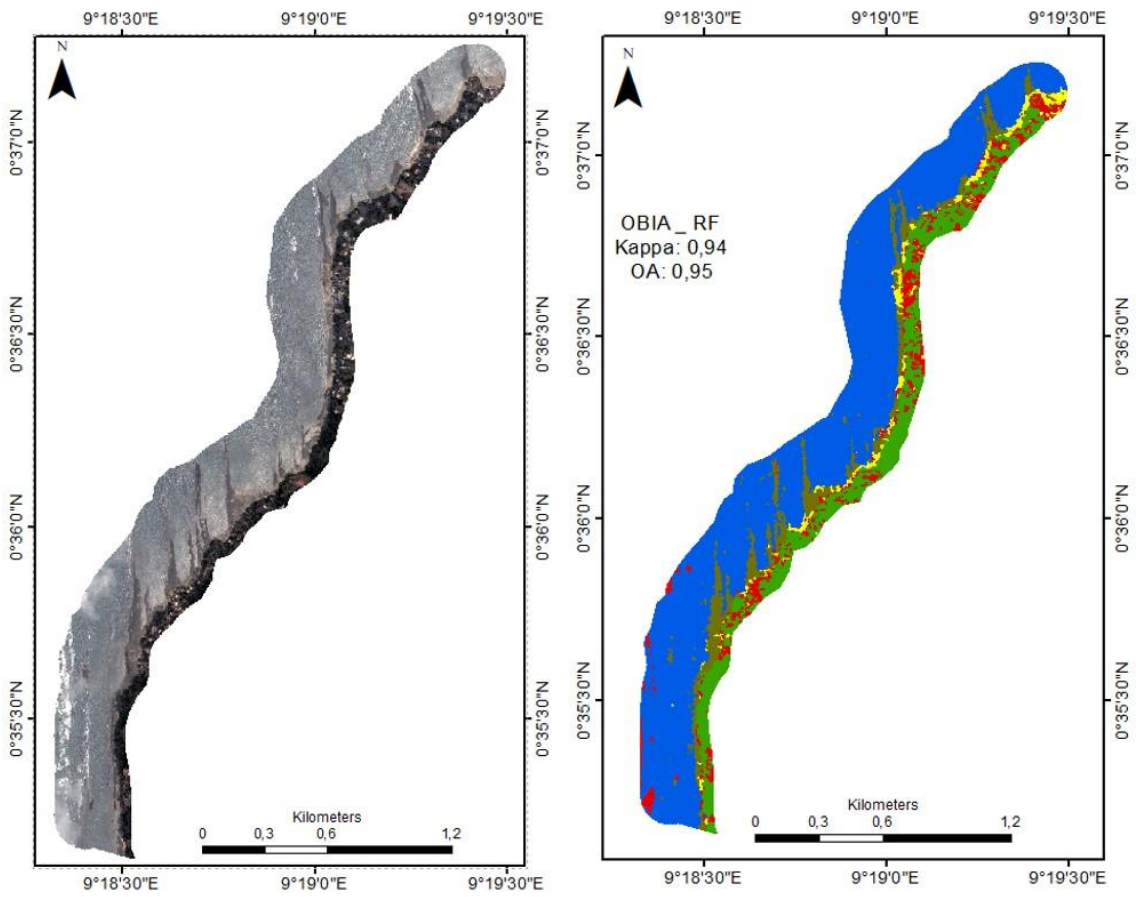

Figure 7: Zone 1 classification by RF-OBIA

The results obtained using the confusion matrix show that the learning rates per class are correct since they are above 90% in most cases. All five classes (water, wet sand, dry sand, vegetation and urban) are represented. The confusion matrix presents slight classification conflicts between the classes "wet sand" and "dry sand" and "dry sand" and "urban". This confusion may arise from the fact that certain pixels of the sand have spectral information similar to certain pixels belonging to the "wet sand". The slight confusion between the two other classes can also be explained by a similarity of spectral signature between dry sand and bare soils included in the "urban" class. Furthermore, it would like to point out that in the majority of cases, the class "wet sand" actually represents the rocky flat which is covered with a thin layer of wet sand. The indicators by class (precision, recall and f-score) are also correct since they are above 90% in most cases.

From these excellent results, the coastline was extracted by converting the polygon vector image into polyline vectors. This made it possible to extract the coastline (Figure 8) by selecting the vegetation and urban classes in the attribute table.

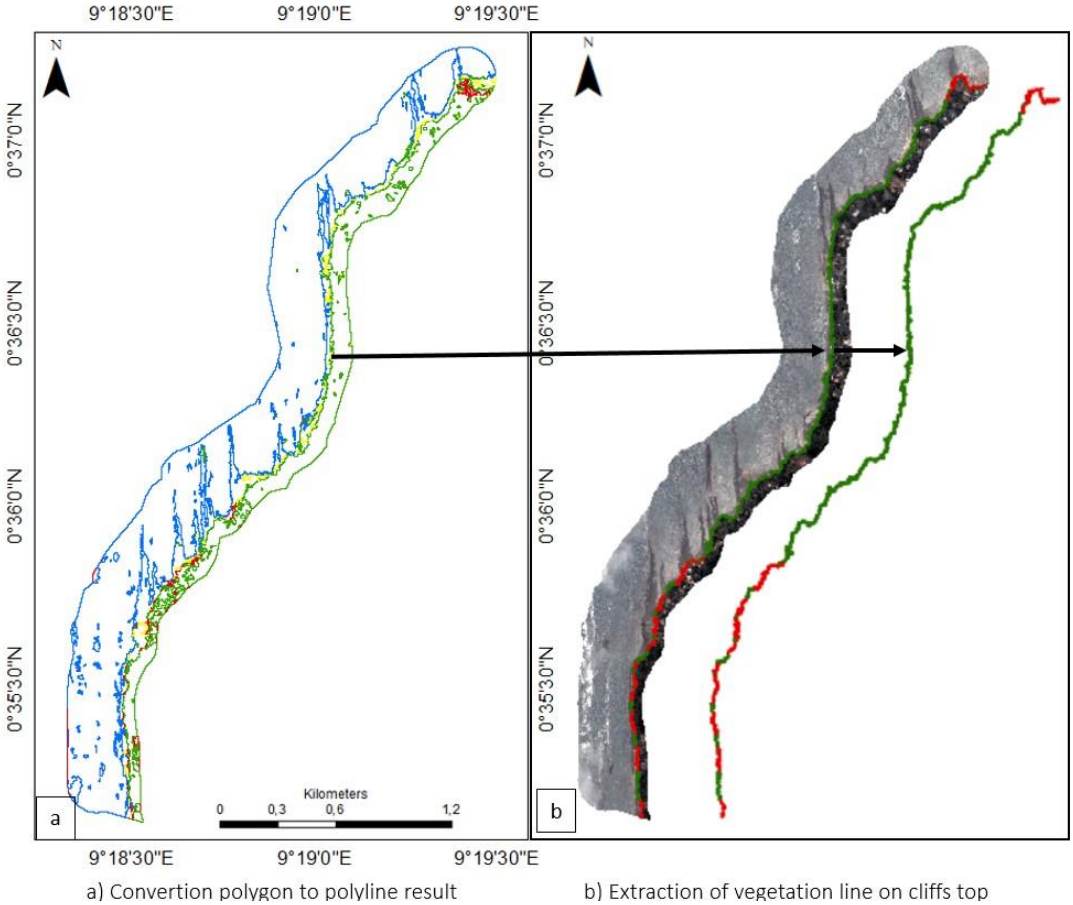

Figure 8: Shoreline extraction by RF-OBIA in zone 1

The coastline extracted is that defined by the limit of the vegetation at the top of the cliffs. The top of the cliffs are not always covered with vegetation. In the rare cases where the vegetation is hindered by built-up areas, the limit on the sea side of the building (barrier) was considered for In addition, the coastal line is also a broken aspect linked to the confusion of classification between vegetation and buildings. It can be seen that there are linear sectors belonging to the "urban" class which encroach on the vegetation in urbane zone. In this case, we consider this linear as a coastline because it reflects the limit of vegetation at the top of the cliffs (Figure 9).

Coastline formed from the merger of two coastline indicators.

Figure 9: Coastline fragmented

As a whole, the coastline does not suffer from any gap (discontinuity) thanks to the fusion of the linear obtained from the "urban" class. In other cases of class confusion between the vegetation and the urban, the limit of the latter has been considered as the coastline (figure 10).

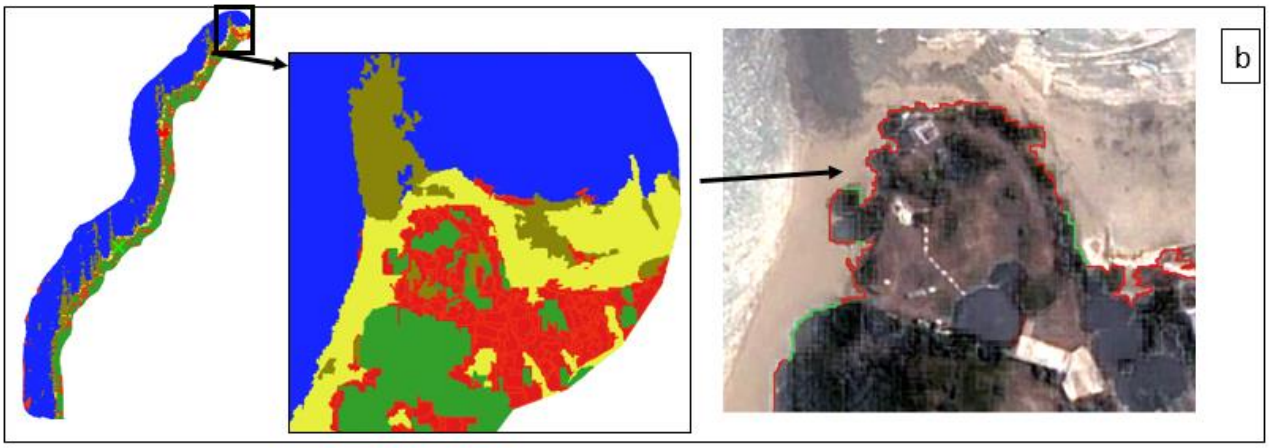

Case of classes confusion

Figure 10: Case of class confusion

The confusion matrix of the classification of test area 2 (Libreville) indicates that the learning rates per class are satisfactory since they are above 80 in general. The five classes (water, wet sand, dry sand, vegetation and urban) were also all extracted (Figure 11). The “urban” class has the lowest classification accuracy rate, at 78%. This rate comes from a confusion between this class and all the other classes. However, the vegetation class causes the most confusion. This confusion may be related to the shade. Because the class "urban" includes buildings and these buildings often generate shade, as well as vegetation (tree).

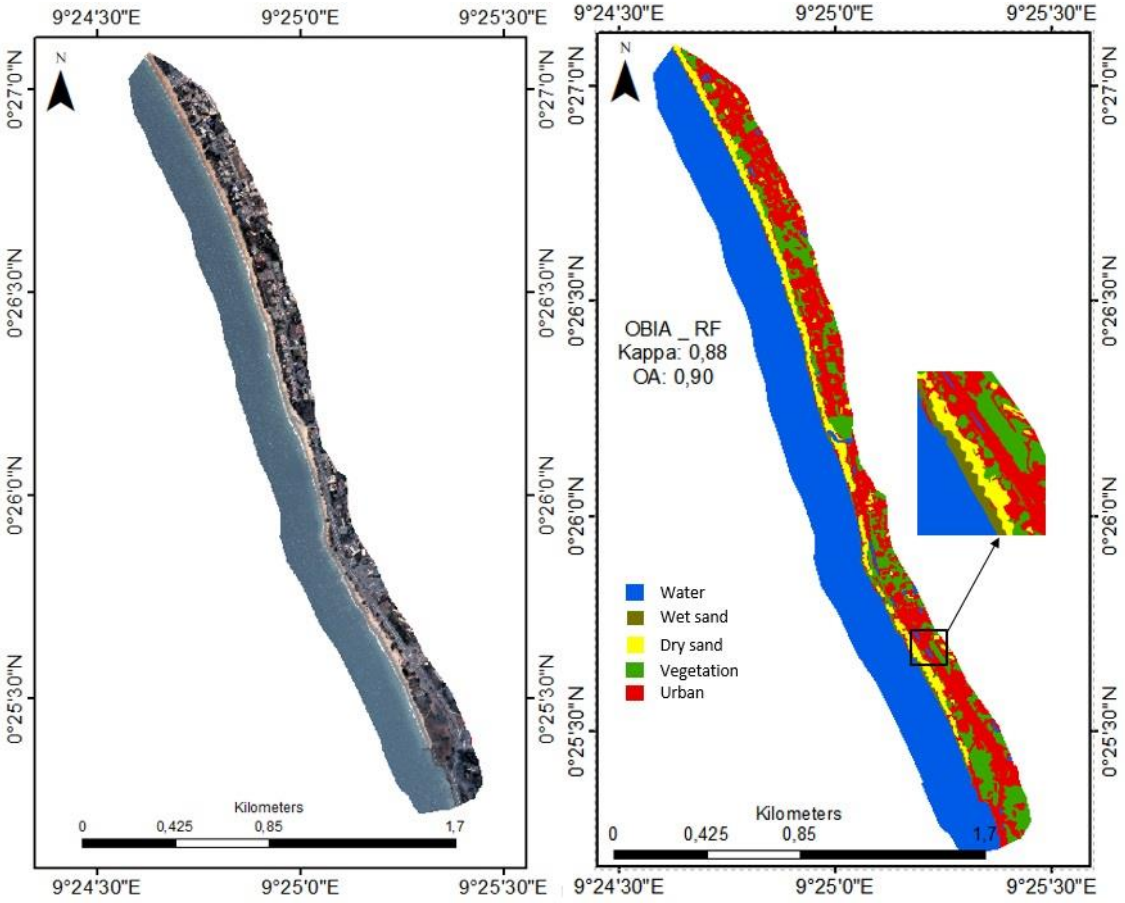

Figure 11: Zone 2 classification by RF-OBIA

The conversion of the polygon vector image into polyline vectors allowed extracting two coastlines. The first is instantaneous water line and the second is wet/dry line or runup maxima (Figure 12). These indicators turned out to be very relevant because the sandy beach makes it visible almost over the entire area of interest. It should be reported that compared the two extracted coastlines, it is the second, which is interrupted, unlike the first, which is a continuous line.

F

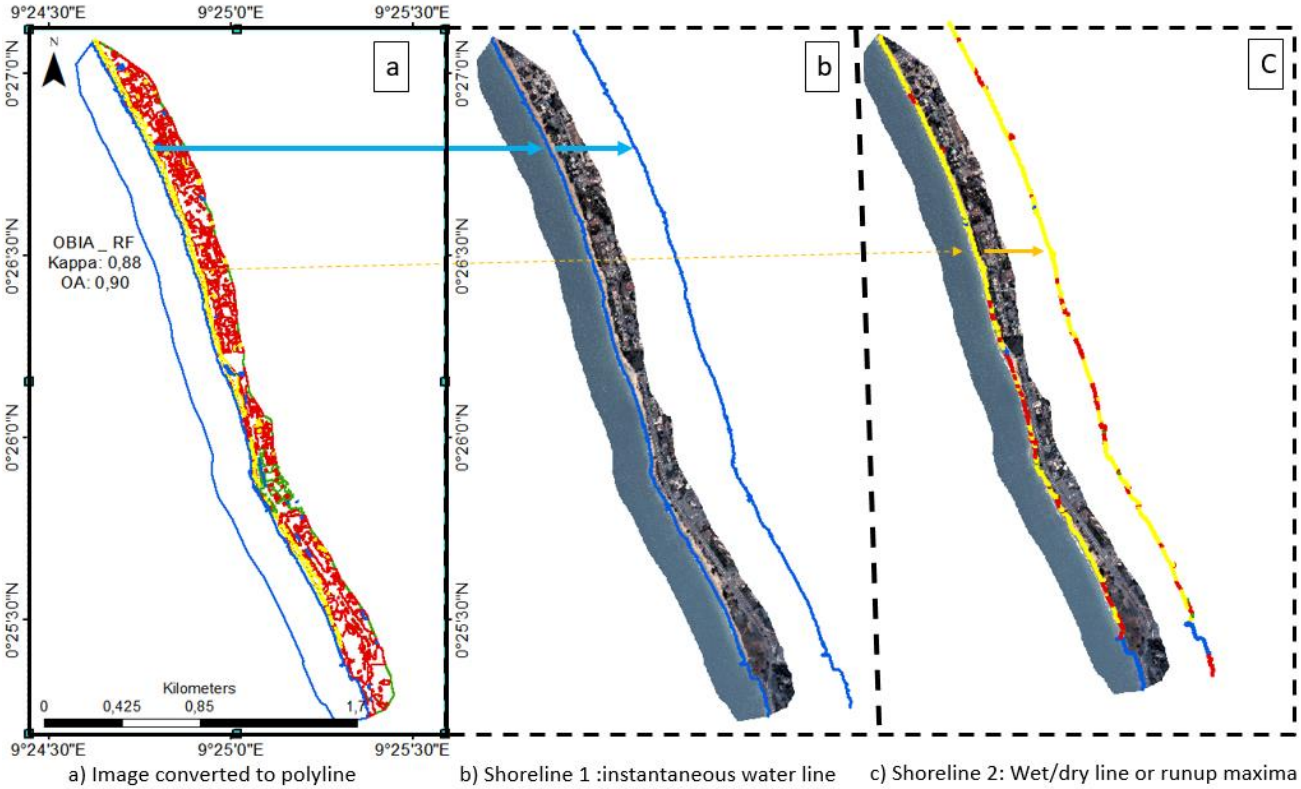

Figure 12: Shoreline extraction by RF-OBIA in zone 2

According to the results of the learning rates obtained for the classification of the image of the third test area located in the municipality of Owendo, the 5 classes of were not correctly extracted (Figure 13). Consequently, the learning rates by class rarely reach the 80% mark, for instance “vegetation” class and “Water” class, which exceed the 80% threshold. The “dry sand” and “urban” classes are my well-ranked classes. Many pixels belonging to the "dry sand" class have been classified as flat to the "wet sand" and "urban" classes.

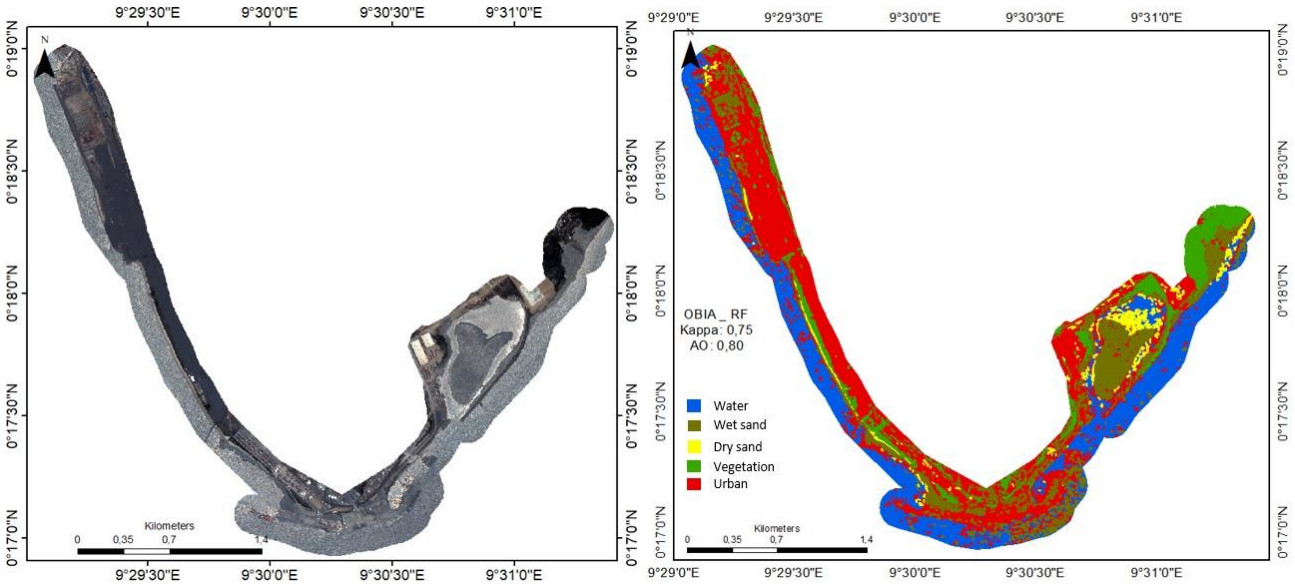

Figure 13: Zone 3 classification by RF-OBIA

May be confusion with the “urban” class comes from the fact that this class also takes into account bare soils whose spectral characteristics would seem similar to those of the “dry sand” class. Moreover, the “urban” class, for its part, merges with almost all the other classes except the “dry sand” class. The "wet sand" and "water" classes have the most biased rates. Indeed, this confusion with the aforementioned first class is linked to the fact that wet bare soils have spectral signatures similar to that of wet mud or sand. It should be noted that the Owendo area has a mostly muddy coast due to the supply of continental sediments to the beaches via the Komo River. It is not entirely fortuitous to recall that the “urban” class includes sub-classes such as: built-up areas, bare soils and all kinds of anthropogenic marks. Thus, note that the quay of Owendo has been "erased" to the detriment of the "water" class.

The reason for this may lie in the fact that the quay in Owendo's port is most likely coated with a thin layer of wet sand at the outset. Additionally, the tide coefficient was at a low point during image acquisition, which could emphasize the turbidity of the seawater and in turn, affect classification by introducing spectral features akin to the dock, ultimately causing confusion between categories.

Considering previous classification results, the extraction stage of the coastal zone was important. Similarly, the polygon vector image was converted to a polyline vector (Figure 14). The coastline used here is derived from a combination of several other reference points: inflow maxima or wet/dry lines, landward edges of coastal structures, and vegetation Limit. The extraction of coastlines heavily relies on their accurate classification, as a flawed categorization renders the extraction process unfeasible. To overcome the challenges posed by the discontinuity of each frame of reference, multiple frames of reference were utilized. Although significant efforts were made to obtain a complete coastal line encompassing the entirety of the study area, errors in classification still resulted in a fragmented appearance.

The primary objective of the classification process is to extract the coastline using various indicators such as the boundary between dry and wet sand, the limit of the run-up, the limit of vegetation or buildings like barriers, riprap, arrows, and the foot of the cliff. To achieve this, the conversion of the image into a polygon vector format had to be transformed into polyline vectors, aligning it with the aforementioned reference lines. The unsmoothed coastline after the conversion from polygon to polyline format is exhibited in figure 14-a. This is merely a rough drawing made to provide a general overview of the coastline. A visual inspection was then performed, confirming that the reference line was clearly recognizable and matched reasonably well with the coastline in the imagery.

Comparing the three classification approaches, we found that ML with RF was more relevant than DL for classifying the three test domains. These areas have same spatial resolutions and topographic features.

The application of RF-OBIA method in test area 1, our objective was achieved very satisfactorily. The classification and extraction of coastlines was facilitated by the fact that there were not many signs of enthronization marks. However, this stretch of coastline has more noise than other areas because it is based on treetop routing. Manual digitization of vegetation (shrubs) requires more time and attention to detail. Being able to do this thanks to the classifications in Rescore is quite a feat. However, a smoothing process is needed to better reflect the actual situation. Cliff areas are often difficult to access, so this approach provides an excellent relief for field data collection, although it is also important for better coastal surveillance.

Furthermore, the second area classification results show that the classification of sandy coastlines can simultaneously extract three coastlines, despite the necessity of a judicious choice of identified classes. As well, the coastlines in question are : the instantaneous limit of the run-up; the boundary between dry sand and wet sand; and, the vegetation line. The coastline defined by the limit of the run-up is the best executed but the least relevant because of its very changing nature over time. The last two, although often discontinuous due to classification errors, are to be preferred for extraction. Visual inspection efforts and adjustments (manual scanning) are still required. As for urbanized areas and muddy foreshore like those of the third zone, their classifications are not satisfactory because the RF model struggles to clearly identify the different objects such as dry sand, wet sand and built-up areas. We can see that only the vegetation class was successfully classified, reaching an accuracy rate of 96%.

Badly classified pixels hinder the recognition of the coastal line in the sense that they do not reflect the reality on the ground but also do not allow the recognition of the coastline. Moreover, if the discontinuous character of the anthropogenic indicators (limit of riprap, residential barriers, retaining walls, etc.) and geomorphological (dry sand, wet sand, foot of cliff) cannot by themselves serve as a definition on several kilometers, they nevertheless serve as a connection in certain places where the vegetation or the limit of the run-up shows these limits, etc. It is difficult to define a coastline in its entirety with only one indicator, unless it is a very small study area. In our three test areas, the vegetation limit seems more suitable for the delimitation of the geomorphological coastline [26] as well as the limit of the run-up are the most represented indicators because of their continuity in space.

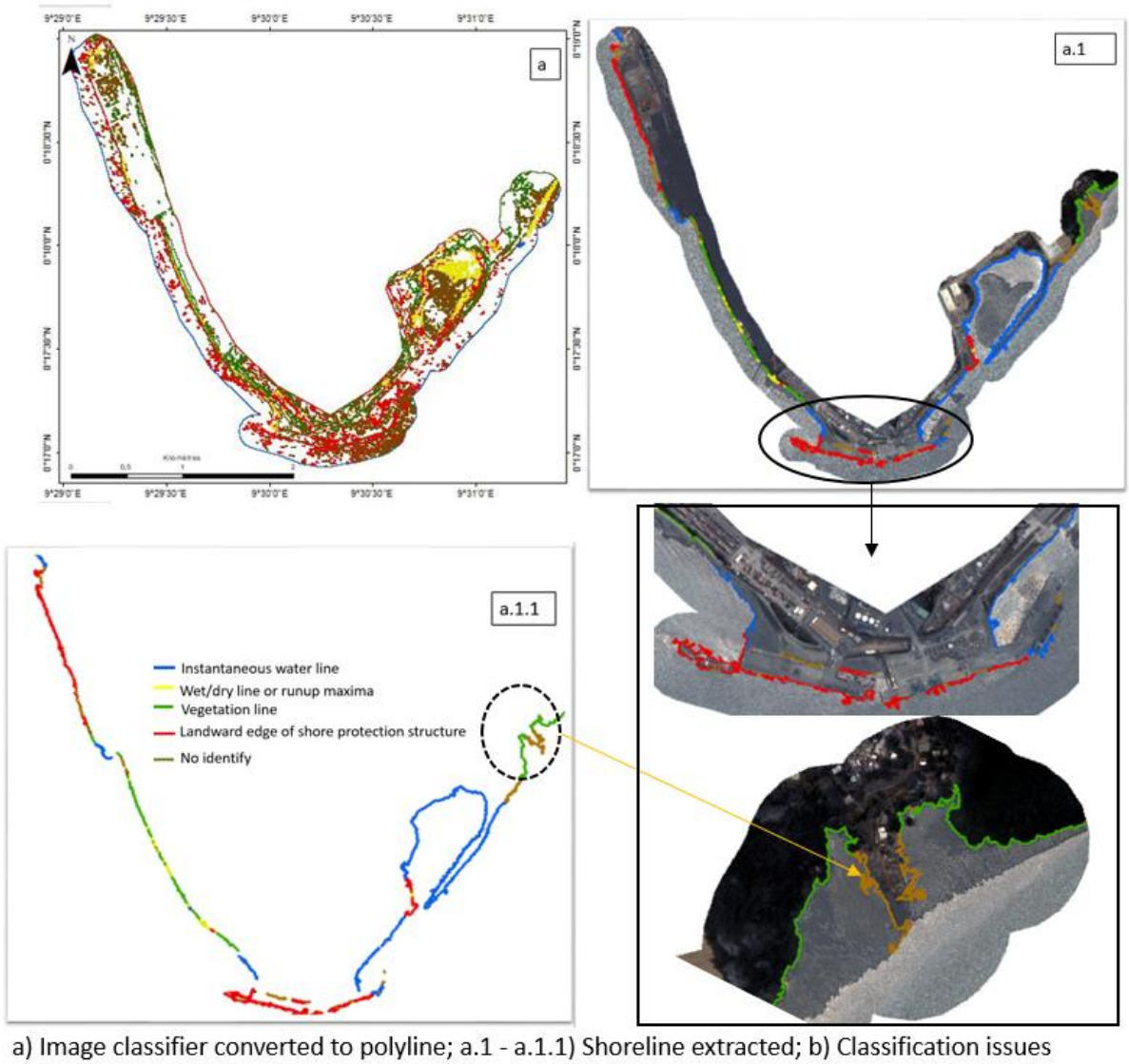

Figure 14: Shorelines extraction by RF-OBIA in zone 3

5. Conclusion

This study entitled "Automatic detection and extraction of the coastline of Greater Libreville (Gabon) using machine learning methods and convolutional neural networks" aimed to find a relevant automation method for the extraction of the feature coast of Greater Libreville. It was used as a spatial data a Pléiades very high resolution (VHR) satellite image acquired on 2022. Three areas of interest were extracted for the satellite images. To reach the primary objective of this study, different Machine and Deep Learning approaches have been tested. For this purpose, PBIA and OBIA approaches based on ML algorithms were performed and compared to the CNN integrated with OBIA approach. As well, three algorithms (RF, SVM and CNN) were examined in three areas located respectively in the municipalities of Akanda, Libreville and Owendo. For the implementation of the different approaches, sampling points (training and

validation) as well as the three extracted satellite images were requested. The selected algorithms allowed to assess the performance of the proposed approaches by creating models that could be used for image classification and validation. Five classes were distinguished for each classified image: ‘water’, ‘wet sand’, ‘dry sand’, ‘vegetation’ and ‘urban’. Fifteen classified images were obtained but only three of them were presented. It is from them that the coastlines were extracted and they were obtained thanks to the OBIA approach driven by the RF. Indeed, the RF-OBIA approach was the most efficient for the detection and the extraction of the coastline. It reached OA and kappa index rates equal to 95% and 94% of the Akanda area; 90% and 88% for the Libreville area and 80% and 75% for the Owendo area. In second position, the SVM then the CNN. Although the classification results were generally satisfactory, after visual inspection and consulting the information provided by the confusion matrix, there is a great confusion of classes coming mainly from the ‘urban’ and ‘dry sand’ classes in the municipality of ’Owendo. These confusions of classes have repercussions on the extraction of the coastline, thus preventing the recognition and extraction of certain indicators in certain sectors where the error is large. Moreover, certain anthropogenic and geomorphological indicators present more limits related to their discontinuities in time, which calls into question their relevance as coastline indicators. Additionally, on the coast, the vegetation limit and the run-up are the most appropriate indicators because of their continuities in space, making the detection, extraction and choice of the latter as reference points less complex. This study showed the relevance of machine learning for the automatic detection and extraction of varied coastlines. Although the latter are very affected by noise due to the fact that the algorithm that generates them processes data in great detail. If, the automation of the coastline proves to be a perfect alternative for the extraction of the coastline in on small scale linear like that of Akanda or Libreville, manual adjustments will be required to improve results.

Acknowledgments

The authors would like to thank CNES (Centre national d'études Spatiales) for the Pléiades image « Pléiades © CNES 2022, Distribution Airbus DS. ICR_FC_378341. This research was funded by the the project CNES (Centre national d'études Spatiales) / TOSCA 7618 / 2022.

Conflicts of interest

The authors declare no conflicts of interest.

6. References

[1] Dalponte, M.; Orka, H.O.; Gobakken, T.; Gianelle, D.; Næsset, E. Tree species classification in boreal forests with hyperspectral data. IEEE Trans. Geosci. Remote Sens. 2012, 51, 2632–2645.

[2] Adam, E.; Mutanga, O.; Odindi, J.; Abdel-Rahman, E.M. Land-use/cover classification in a heterogeneous coastal landscape using RapidEye imagery: Evaluating the performance of random forest and support vector machines classifiers. Int. J. Remote Sens. 2014, 35, 3440–3458.

[3] Maxwell, A.; Warner, T.; Strager, M.; Conley, J.; Sharp, A. Assessing machine-learning algorithms and image-and lidar-derived variables for GEOBIA classification of mining and mine reclamation. Int. J. Remote Sens. 2015, 36, 954–978

[4] Raczko, E.; Zagajewski, B. Comparison of support vector machine, random forest and neural network classifiers for tree species classification on airborne hyperspectral APEX images. Eur. J. Remote Sens. 2017, 50, 144–154.

[5] Soumia Bengoufa, Simona Niculescu, Mustapha Kamel Mihoubi, Rabah Belkessa, Ali Rami, Walid Rabehi, and Katia Abbad. 2021. Machine learning and shoreline monitoring using optical satellite images: case study of the mostaganem shoreline, algeria. Journal of applied remote sensing, 15(2):026509.

[6] Abdel-Rahman, E.M.; Mutanga, O.; Adam, E.; Ismail, R. Detecting Sirex noctilio grey-attacked and lightning-struck pine trees using airborne hyperspectral data, random forest and support vector machines classifiers. ISPRS J. Photogramm. Remote Sens. 2014, 88, 48–59

[7] Shang, X.; Chisholm, L.A. Classification of Australian native forest species using hyperspectral remote sensing and machinelearning classification algorithms. IEEE J. Sel. Top. Appl. Earth Obs. Remote Sens. 2013, 7, 2481–2489

[8] Lawrence, R.L.; Moran, C.J. The AmericaView classification methods accuracy comparison project: A rigorous approach for model selection. Remote Sens. Environ. 2015, 170, 115–120

[9] Yoo C., Han D., Im J., Bechtel B. Comparison between convolutional neural networks and random forest for local climate zone classification in mega urban areas using landsat images. ISPRS J. Photogram. Rem. Sens. 2019;157:155–170.

[10] Xie, G.; Niculescu, S. Mapping and Monitoring of Land Cover/Land Use (LCLU) Changes in the Crozon Peninsula (Brittany, France) from 2007 to 2018 by Machine Learning Algorithms (Support Vector Machine, Random Forest, and Convolutional Neural Network) and by Post-classification Comparison (PCC). Remote Sens. 2021, 13, 3899.

[11] Boak E. H., Turner I. L. (2005) Shoreline definition and detection: A review. Journal of Coastal Research, vol. 21, n°4, p. 688 - 703.

[12] Zaabar, N., Niculescu S. and Kamel, M. M. 2022. "Application of convolutional neural networks with object-based Image Analysis for Land Cover and Land Use Mapping in Coastal areas: a case study in ain témouchent, Algeria," In IEEE Journal of selected topics in Applied Earth Observations and Remote Sensing, vol. 15, pp. 5177-5189, Doi: 10.1109/jstars.2022.3185185.

[13] Baatz, M. and Schape, A., 2000. Multiresolution segmentation: an optimization approach for high quality multi-scale image segmentation. In: strobl, j., blaschke, t. And griesbner, g., eds., angewandte geographische informations-verarbeitung, xii, wichmann verlag, karlsruhe, germany, 12-23.

[14] Rodriguez-Galiano V.F; Chica-Olmo M. and Chica-Rivas M. (2014) Predictive modelong of gold potential with the integration based on random forest: a case study on the Rodalquilar area, Southern Spain, International Journal of Geographical Information Science, 28:7, 1336-1354, DOI: 10.1080/13658816.2014885527

[15] Breiman, L. Random forests. Mach. Learn. 2001, 45, 5–32.

[16] Ghosh, A.; Fassnacht, FE; Joshi, Pk ; Koch, B. Ramework for mapping tree species combining hyperspectral and lidar data: role of oelected classifiers and sensor across three spatial scales. int. J. Appl. Earth Obs. Geoinf. 2014, 26, 49–63.

[17] Belgiu, M.; Dragut, L. Random forest in remote sensing: a review of applications and future directions. isprs j. photogramm.remote sens. 2016, 114, 24–31.

[18] Guan, H.; Li, J.; Chapman, M.; Deng, F.; Ji, Z.; Yang, X. Integration of orthoimagery and lidar data for object-based urban thematic mapping using random forests. Int. J. Remote Sens. 2013, 34, 5166–5186

[19] Vapnik, V. (1998) Statistical Learning Theory. John Wiley & Sons, Chichester

[20] Devadas,R. ; Denham, R. ; and Pringle, M. ; "Support vector machine classification of objectbased data for crop mapping, using multi-temporal Landsat imagery," Int. Arch. Photogramm. Remote Sens. Spatial Inf. Sci. XXXIX-B7, 185–190 (2012)

[21] Zainib Noshad et al., Fault Detection in Wireless Sensor Networks through the Random Forest Classifier, 1 April 2019

[22] Ghorbanzadeh, O. and Blaschke, T., 2019. « Optimizing Sample Patches Selection of CNN to Improve the mIOU on Landslide Detection »:, in Proceedings of the 5th International Conference on Geographical Information Systems Theory, bApplications and Management, Heraklion, Crete, Greece, p. 33-40. doi: 10.5220/0007675300330040.

[23] Baatz, M. and Schape, A., 2000. Multiresolution Segmentation: an Optimization Approach for High Quality Multi-Scale Image Segmentation. In: Strobl, J., Blaschke, T. and Griesbner, G., Eds., Angewandte Geographische Informations-Verarbeitung, XII, Wichmann Verlag, Karlsruhe, Germany, 12-23

[24] Thanh Noi, P. and Kappas, M. (2017) Comparison of Random Forest, k-Nearest Neighbor, and Support Vector Machine Classifiers for Land Cover Classification Using Sentinel-2 Imagery. Sensors (Basel), 18, 18

[25] Jensen, JR ; Lulla, K. Traitement d'image numérique d'introduction : Une perspective de télédétection.Géocarto Int.1987,2, 65.

[26] LEBERRE (I.), HENAFF (A.), WENZEL (F.), GIRAUDET (J.), 2004. – *Cartographie synthétique de l'environnement littoral du Finistère, exploitation de SPOT pour la cartographie de l'estran, du trait de côte et de l'occupation du littoral*, Rapport final, Appel à proposition CNES/IFEN « Suivi du littoral par SPOT5 », laboratoire Géomer/Cetmef/DDE29, 108